DNA Binding to an Anticancer Organo-Ruthenium Complex

Marcelina Klajner,[†,‡] Pascal Hebraud,[†] Claude Sirlin,[§] Christian Gaiddon,[||] and Sebastien Harlepp*[,†]

I.P.C.M.S., UMR7504, Université de Strasbourg, France, Wrocław University of Technology, Poland, Institut de Chimie, C.N.R.S., UMR7177, Université de Strasbourg, Synthèses Métallo-Induites, France, and INSERM U692-Université de Strasbourg, Signalisations Moléculaires et Neurodégénérescence, France

Received: May 17, 2010; Revised Manuscript Received: September 16, 2010

Because many anticancer drugs interact with DNA, the determination of their association constants to DNA is essential for quantifying their mechanisms of action. The interactions between a new ruthenium-derived compound [ruthenium(phenanthroline)(κ-*C*,*N*-(2-phenyl-pyridine)$(NCMe)_2$]PF_6, called RDC11] and DNA are studied using different techniques. Fluorescent experiments are used to determine the association and dissociation constants under different salt concentrations. The binding is shown to be reversible and noncovalent. The association constants vary from 1.5×10^6 M^{-1} to 2.9×10^3 M^{-1} when increasing the sodium concentration from 0.1 to 200 mM. Single-molecule stretching methods are used to study the interaction of RDC with longer DNA strands (8.6 kbp home-built dimer of pBR322). The affinities of RDC with DNA under different loads are obtained using McGhee and von Hippel analysis. The affinity constant and thermodynamic parameters are in good agreement with the values found in the literature and lead to the conclusion that this molecule intercalates dsDNA.

Introduction

Inorganic compounds have an enormous impact in medicine, particularly, in the treatment of cancer. Rosenberg's[1,2] discovery of cisplatin and its subsequent clinical use is well-documented.[3] Cisplatin continues to be used in 50−70% of all patients suffering from cancer, usually in combination with other drugs. It is especially effective in treating testicular[4] and ovarian[5] carcinoma but is also used to treat other types of cancers.[6] Although cisplatin is arguably the most successful anticancer drug in the world, it is not without flaws. It exhibits a high general toxicity leading to undesirable side effects[7,8] that can be minimized by careful administration[9,10] and is inactive against many cancer cell lines and metastases (secondary cancers).

Several studies showed that organometallic molecules containing ruthenium have promising anticancer characteristics.[11−17] A variety of molecules containing ruthenium Ru(II) or Ru(III) have been synthesized and tested for their biological functions.[18,19] These molecules exhibit cytotoxicity against cancer cells and present ligand-exchange abilities analogous to those of platinum complexes.[11,20−24] They have also been shown to reduce tumor growth in animal models.[17,25−29] Furthermore, these ruthenium-containing drugs often avoid the drawback of current anticancer drugs.[17] In contrast to platinum drugs,[30] ruthenium-containing drugs are not sensitive to resistance mechanisms and seem to have less side effects on healthy tissues because they can use the iron detoxification paths inside the body.[11,17,21,31,32]

Determining the changes in DNA structure and dynamics induced by ruthenium-derived compounds (RDCs) is essential to elucidate the specific mechanism by which they function. The basic pattern, a Ru(II) center surrounded by three heterocyclic, aromatic, bidentate ligands, has provided a convenient three-dimensional scaffold for building a family of complexes with different shapes, sizes, functional groups, and properties. In general, these complexes bind noncovalently to DNA by a combination of electrostatic and van der Waals effects, but their binding constants, exchange rates, and details of interaction with DNA vary. It has been reported that depending on the structure and chemicals surrounding ruthenium, these molecules bind intercalatively and/or electrostatically (i.e., nonintercalatively in one of the DNA grooves).[33] To date, a majority of the reported ruthenium-containing molecules interact with DNA and cause DNA damages in cancer cells.[34,35] The mode of interaction with DNA varies depending on the structure of the molecule and can involve intercalation,[36] cross-linking,[37] and ionic interactions.[38] In this article, we will discuss one of these complexes, that has shown anticancer activity:[17,39,40] RDC11[ruthenium-(phenanthroline)(κ-*C*,*N*-(2-phenyl-pyridine)$(NCMe)_2$]PF_6.

RDC11 has already been explored at the cellular level,[17] and an increase of cancer cell mortality was observed on B16F10, U87, and TK6 cell lines in vitro.[17] Motivated by the idea that the binding of RDC11 with DNA plays a role in its mechanism of action, we study the affinity and the interaction mode of this compound with nucleic acids. The binding of this RDC11 complex to DNA is explored using Förster resonant energy transfer (FRET) microscopy and force extension measurements by optical tweezers. These two techniques have unique operational principles and measure different properties of DNA. As a result, each has the potential to provide unique information about the binding of RDC11 complexes. For instance, when an intercalator binds, DNA opens up and unwinds to accommodate it between the base pairs. In the process, the DNA helix gets longer, whereas for a minor groove binder, there will be a reduction or no changes in DNA length.[41−43] Thus, if we measure the length of a piece of DNA, add a molecule of interest, and observe that the DNA gets longer, we can conclude that this molecule is an intercalator. The increase in DNA length

* To whom correspondence should be addressed. E-mail: harlepp@ipcms.u-strasbg.fr.
[†] UMR7504, Université de Strasbourg.
[‡] Wrocław University of Technology.
[§] UMR7177, Université de Strasbourg.
[||] INSERM U692-Université de Strasbourg.

10.1021/jp1044783
Published on Web 10/20/2010

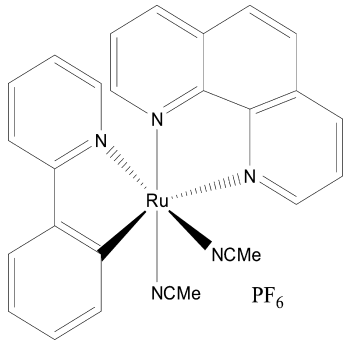

Figure 1. Stereochemical representation of RDC11 (mixture of two racemic enantiomers).

is directly related to the number of molecules that bind to a piece of DNA and thus can be used to determine the binding constant. A sensitive tool used to measure distance changes at the nanometric scale is FRET, which exploits a strong donor−acceptor distance dependence (R^{-6}). FRET has been extensively used to study different nucleic acid forms, for example, A-, B-, and Z-DNA,[44,45] quadruplexes,[46] four-way junctions,[47] hairpins,[48] single-stranded DNAs,[49] and catalytic RNAs.[50] Because of its sensitivity, this technique is well-suited for probing specific and nonspecific interactions between DNA and ligands and to determine both the affinity constant and the Hill constant.[51] In our case, we made bulk experiments where orientation is averaged over all of the equiprobable conformations, and the only remaining parameter in this system is the distance separating the donor from the acceptor. Small variations in DNA conformations cause changes in the donor−acceptor coupling and consequently on the efficiency of FRET measurements. These changes are then translated into a change in length.[52] Generally, when a chemical compound interacts with DNA, the mechanical properties of the latter change.[53] Thus, techniques that measure the mechanical behavior of the two DNA strands can also provide relevant information about the binding of molecules to DNA. Optical tweezers have been used previously to stretch single molecules of double-stranded DNA. They allow us to measure the contour length of the DNA and the forces required to pull the two DNA strands apart, thereby elucidating DNA binding and stabilization by various proteins and ions.[54,55] DNA stretching has also been used successfully to examine binding by simple intercalators and groove binders.[53] In this work, we have one specific goal in mind when using bulk and single molecule experiments. In bulk, we follow the general picture of interactions. We can tell about the general changes in the structure of DNA, about the nature of the bond formed (covalent or not), and explore the dependence on the concentration of salt. In contrast at the single molecule level, we should find out more about the specificity of the interaction (intercalation, electrostatic, etc.). The complementarity of these techniques is thus expected to lead to a general understanding of the interaction (Figure 1).

Materials and Methods

Sample Preparation. ***RDC11.*** [Ruthenium(phenanthroline)-(κ-*C*,*N*-(2-phenyl-pyridine)(NCMe)$_2$]PF_6 was synthesized in a two-step process. Phenyl-pyridine was first cyclometalated by reacting with the Ru(η^6-C_6H_6)Cl_2 dimer in acetonitrile. The second step consists in an exchange of two acetonitrile against one phenanthroline ligand leading to the target complex.[39,40] The final product is a mixture of two racemic enantiomers in the cis position, and the carbon is in the trans position as compared to the nitrogen.[40] A stock solution of 40 mM was prepared by dissolving in dimethylsulfoxide. Dilutions of RDC11 were performed in the same buffer as the one containing the DNA samples.

DNA for FRET. The measurements were performed with 15 base pair duplex DNA. Complementary strands were purchased from IBA NAPS with sequences: GGA GAC CAG AGG CCT and AGG CCT CTG GTC TCC. We chose this sequence because it had been previously used in cisplatin activity studies.[56] The first sequence was 5′-labeled with Alexa488 and 3′-labeled with Alexa568. This labeling was ensured directly by IBA with a PAGE purification. The distance at which this fluorophore pair undergoes 50% energy transfer, R_0, has been measured to be 62 Å.[57] The two strands were resuspended with a final NaCl concentration of 100 μM. The two strands were combined at an equal molar concentration of 8.3 μM and were annealed by heating the DNA to 94 °C before cooling down the sample to 16 °C in 20 min. All measurements with 100 μM NaCl were done at 20 °C or less to ensure that the DNA remained fully annealed. This was checked with the FRET activity, which remains equal to 76% when DNA is double-stranded and increases to 95% when DNA is single-stranded. At higher salt concentrations, the DNA was diluted into 200 μM Tris-HCl (pH 8.0 at 25 °C) and 200 μM KCl. We further increased the salinity with sodium chloride.

DNA for Optical Trapping. An *Eco*RI linearized pBR322 plasmid was labeled with biotin or digoxigenin. We obtained two differently labeled types of DNA and applied to each of them a *Hin*dIII restriction. We purified this restriction product to keep only the 4.3 kb DNA. A final ligation between the two different DNA types led us to a 50% concentration of a pBR322 dimer colabeled with biotin and digoxigenin. A first incubation with 1 μm streptavidin beads, followed by a second with an antidigoxigenin-coated coverslip, resulted in the assembly of a molecular jokari.

Initially coated with aminosilane (Sigma-Aldrich), the coverslips were next treated with glutaraldehyde (50% Electron Microscopy Sciences). It was followed by antidigoxigenin (50 μg/mL, Roche) incubation. To prevent nonspecific binding, we finally used bovine serum albumin (2% VWR). All experiments were performed at 20 °C, and the incubation of all of the chemicals was done in PBS1X. Once the protein ends were attached to the surface, we performed the required buffer exchanges through a flow cell.

Chemical Analysis. Although RDC molecules are smaller than most of the proteins, once absorbed, they may occupy more then one DNA base pair. As a consequence, even in the absence of cooperative effects, once a first RDC molecule is absorbed onto the double strand, the number of conformations of binding neighboring base pairs with RDC is reduced. This effect is not described by standard chemical analysis, such as the Scatchard plot.[58] Following the approach of McGhee and von Hippel (MGVH),[59] we thus write

$$\mathrm{DNA_{bp}} + \mathrm{RDC} \overset{K_a}{\rightleftharpoons} \mathrm{DNA_{bp}RDC}$$

$$K_a = \frac{[\mathrm{DNA_{bp}RDC}]}{[\mathrm{DNA_{bp}}][\mathrm{RDC}]} \quad (1)$$

where [DNA_{bp}] denotes the concentration of DNA base pair and [RDC] denotes the concentration of RDC. Following MGVH, we denote ν the ratio of bound RDC per DNA bp:

$$\nu = \frac{[\mathrm{RDC_b}]}{[\mathrm{DNA_{bp}}]} \tag{2}$$

where $[RDC_b]$ is the molar concentration of RDC bound to dsDNA and $[DNA_{bp}]$ is the total concentration of DNA bp. Following MGVH, the equilibrium condition is

$$\frac{\nu}{[\mathrm{RDC}]} = K_a \frac{(1 - p\nu)^p}{[1 - (p-1)\nu]^{p-1}} \tag{3}$$

where p is the number of DNA bases occupied by a single RDC molecule.

For $p = 1$, one recovers the equilibrium condition given by standard thermodynamics

$$\frac{\nu}{[\mathrm{RDC}]} = K_a(1 - \nu) \tag{4}$$

From the equilibrium condition (eq 3), we determine the affinity constant K_a and the number of sites p occupied by an RDC molecule. K_a is given by

$$K_a = \lim_{\nu \to 0} \frac{\nu}{[\mathrm{RDC}]}$$

and p is given by

$$p = \frac{1}{2} - \frac{1}{2K_a} \lim_{\nu \to 0} \frac{\partial}{\partial \nu} \frac{\nu}{[\mathrm{RDC}]}$$

FRET Microscopy. The fluorescence measurements were performed in a dark room with a custom built microscope (Figure 2). A solid state laser (Coherent 488 Sapphire) excited the donor. The donor emission was collected with a photomultiplier (Hamamatsu H7421 Photon Counting Head), while the acceptor emission was collected with an avalanche photodiode (Perkin-Elmer SPCM-AQR-100). The use of these two different detectors is due to the quantum efficiencies that are optimized for the collected wavelengths. The FRET efficiency, Q, was determined from the ratio of the acceptor emission to the sum of the donor and the acceptor emissions. The data acquisition was controlled with Labview (National Instruments) with an acquisition rate of 5 Hz. At this rate, fluctuations in the fluorescence emission are dominated by the photon noise, which scales as the square root of the signal. By integrating over a period of 200 ms, we collected enough photons so that the signal-to-noise ratio is high (around 50).

Before performing each measurement, we first calibrated the system with the duplex DNA. The FRET efficiencies were always 76%, the expected efficiency for this fluorescent labeled DNA (15 × 0.34 nm gives an efficiency of 76%). Then, we added the right amount of RDC11 and incubated it for several minutes to an hour to reach the equilibrium. A 10 min trace was acquired from both channels, and the mean efficiency and standard deviation were determined. We repeated this operation for each of the data points to build the titration curve.

Optical Trapping Microscopy. The polarized infrared laser beam passed the dichroic mirror and fed the back aperture of the oil immersion objective (Zeiss 100/1.4). The focused beam formed an optical trap for a dielectric particle. Single beam optical tweezers were used to stretch a dimer of pBR322 (see

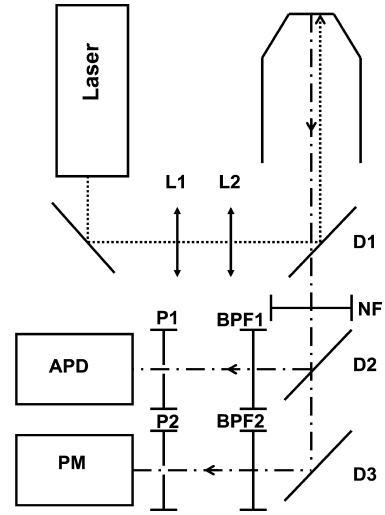

Figure 2. Scheme of setup. Laser (Coherent 488 Sapphire); BPF1 and BPF2 bandpass filters; L1L2 telescope; D1, D2, and D3 dichroic mirrors; NF notch filter; P1 and P2 pinholes; APD (avalanche photodiode, Perkin-Elmer SPCM-AQR-100); and PM (photomultiplier, Hamamatsu H7421).

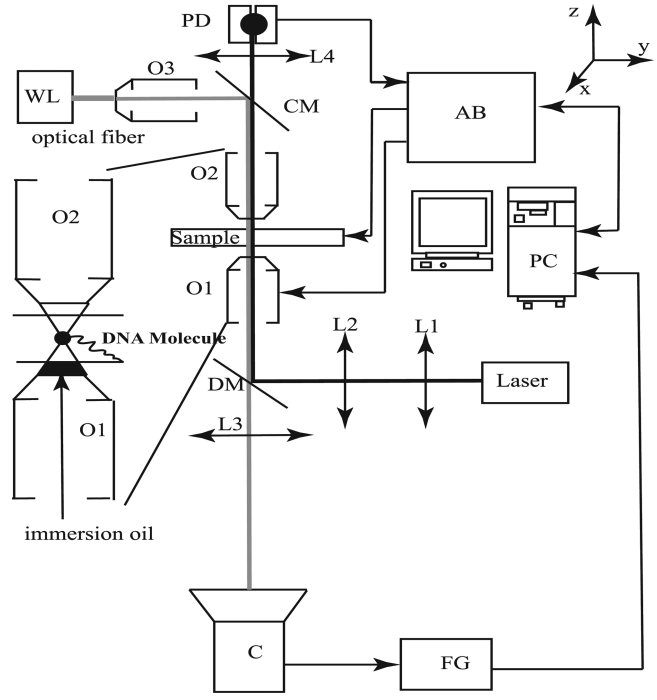

Figure 3. Optical tweezers setup. Trapping path: Laser Millenia YAG 1064 nm, L1L2 telescope, DM dichroic mirror, O1 objective 1 (100× NA 1.3), O2 objective 2 (60× NA 0.6), L4 imaging lens, and PD position diode. Imaging path: WL white light, O3 objective 3 (20× NA 0.3), CM cold mirror, and C. CCD camera. Signal acquisition: FG frame grabber, AB acquisition board (NI6135), and PC personal computer.

the Materials and Methods), which had been labeled with biotin and digoxigenin on the 3′- and 5′-ends. A single DNA molecule was caught in the optical trap (Figure 3). All of the stretching experiments were performed at a pulling rate of 500 nm/s in water or PBS buffer. Solutions containing various RDC11 concentrations were exchanged with buffer surrounding a single DNA molecule to investigate RDC effects on DNA stretching curves. We stretched the DNA through the force-induced melting plateau and then relaxed it to its initial position by moving the piezo-electric stage. Before RDC11 was adding, we

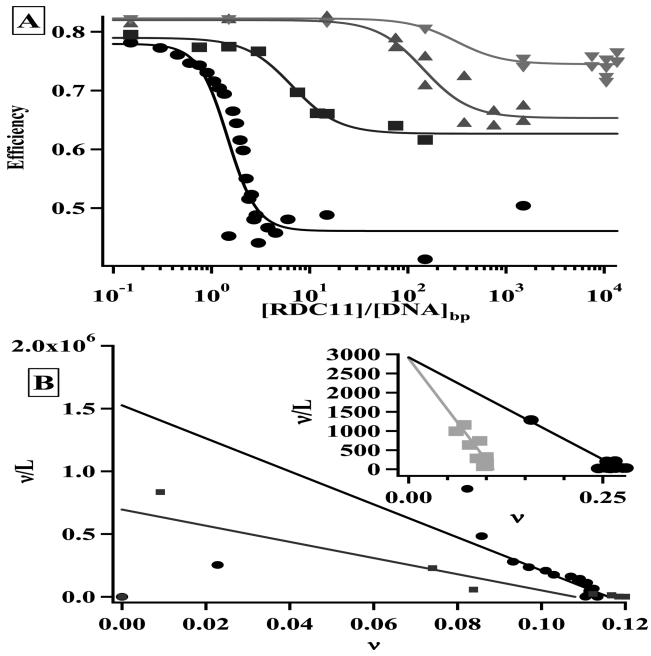

Figure 4. (A) Fret efficiency as a function of RDC11 added at different NaCl concentrations. Key: circle, water; square, 2 mM; triangle, 20 mM; and triangle down, 200 mM. (B) McGhee Von Hippel graph and fitting curves obtained from panel A. For clarity, data obtained for NaCl concentrations equal to 20 and 200 mM are plotted in the inset. The association constants obtained are 1.5×10^6 M^{-1} in water, 6.9×10^5 M^{-1} at 2 mM, 2921 M^{-1} at 20 mM, and 2893 M^{-1} at 200 mM.

first checked the force−extension curve of single DNA molecules and compared the resulting curves with the wormlike chain predictions in different salt concentrations.

The analysis of the stretching curves at different ruthenium concentration was performed as follows. In the case of an intercalant, for forces higher than 10 pN, the extension of an intercalated DNA would be longer than that of a nonintercalated dsDNA. The determination of the fractional number $\gamma_F(C)$ of the intercalant per base pairs was directly related to this change in extension by:

$$\gamma_F(C) = \frac{x(F, C) - x_{ds}(F, 0)}{x_{ds}(F, 0)} \quad (5)$$

where $x_{ds}(F, 0)$ is the elongation per base pair of the dsDNA in the absence of RDCs at the force F and $x(F, C)$ is the elongation of the dsDNA at the force F in the presence of the concentration C of RDCs. Again, we could use the MGVH binding isotherm to fit the curve:

$$\gamma_F(C) = K_F \times C \times \frac{(1 - n_F\gamma_F)^{n_F}}{[1 - (n_F - 1)\gamma_F]^{n_F - 1}} \quad (6)$$

where K_F is the association constant at the given force and n_F represents the occupancy site in DNA base pairs. The association constant depends on the exerted force because once the molecule is lengthened, the energy cost to interact is changed.

Results

Affinities and Dependence on Salt Concentration. The FRET efficiency is plotted in Figure 4A. The efficiency drops from 0.76 to 0.46 as the relative concentration of RDC11 to DNA bp is increased from 0.5 to 3. When the plateau value was reached at high RDC concentration, it meant that all of the DNA strands were saturated with RDC. The FRET efficiency was $R_\infty = 0.46$. In contrast, for free DNA solutions, $R_0 = 0.76$. We plotted ν/L as a function of ν and adjusted the curve with eq 6 to determine the affinity constant K_a and the occupancy size in base pairs p. We obtained an affinity constant of 1.5×10^6 M^{-1} for RDC11 in low ionic conditions (0.1 mM). This value shows that RDC11 binds very tightly to DNA in the absence of counterions.

The high binding affinity under low ionic conditions suggests that RDC11 binds to DNA by electrostatic interactions. We measured the binding affinity of RDC11 as a function of the monovalent salt concentration. We first determined how the FRET efficiency changes as a function of NaCl concentration in the absence of RDC11. We found that the efficiency of naked DNA moves to higher values, which is in agreement with a previous study,[60] which showed that the persistence length of DNA decreases with the addition of monovalent ions. This allows the DNA molecule to bend more, and the average distance between the DNA extremities is diminished. We then carried out RDC11 titrations for increasing concentrations of NaCl (Figure 4A). We observed a decrease in the affinity of RDC for DNA. In water, the half reaction RDC11/DNA ratio was around 1, whereas in 200 mM of NaCl, this ratio became 300 mM. Moreover, the plateau value of the efficiency increased from 0.45 in pure water to only 0.75 in 200 mM NaCl, which indicates that the DNA is less deformed by RDC11 as electrostatic interactions are screened.

The corresponding results are given in Figure 4B. The adjustment of these curves with eq 6 shows that the affinity constant decreases with the addition of salt from $K_a = 10^6$ at 10^{-4} M to $K_a = 10^3$ at 200 mM. The occupancy span of ruthenium to DNA base pairs is around 8 except for the case of 200 mM where the occupancy size drops to 4. By plotting the logarithm of the variation of the affinity constant K_a as a function of the logarithm of the salt concentration, we observe a linear relationship with a slope of +1. Such a result is in agreement with Braunlin's observations,[61] for the affinity of spermine for DNA. He showed that the affinity constant decreases as the n-th power of the added salt concentration, where n is the valence of the binder. In our case, RDC11 has a valence equal to +1.

Reversibility. To verify that the interaction is not covalent, we performed a reverse titration. We mixed RDC and labeled DNA in an equimolar concentration (in bp of DNA) before adding nonlabeled DNA to the solution. The buffer used contains 2 mM salt. We followed the efficiency as a function of the concentration of the added unlabeled DNA. Figure 5 shows the dependence of the efficiency to this added DNA and how the efficiency increases again to close to its initial conditions.

The efficiency increases from 0.65 to 0.75 at high nonlabeled DNA. Because the efficiency came back to the starting level, there was a chemical equilibrium and the addition of DNA moved this equilibrium to lower amounts of bound ruthenium. Hence, the interaction was not a covalent binding, which differs from cisplatin where cross-linking appears. Again, we could extract the dissociation constant using MGVH equation, and its value is 300 nM.

These results unambiguously show that RDC11 exhibits a strong affinity for DNA. The interaction of RDC with DNA is at least in part electrostatic since it is screened by the addition

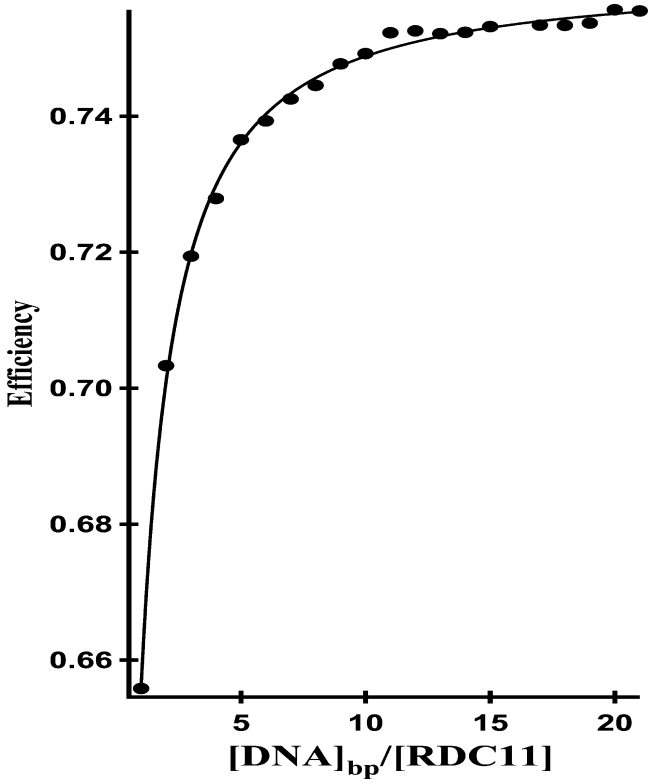

Figure 5. Dissociation of RDC11 from DNA strands as a function of the amount of DNA. The resulting dissociation constant is $K_d = 300$ nM.

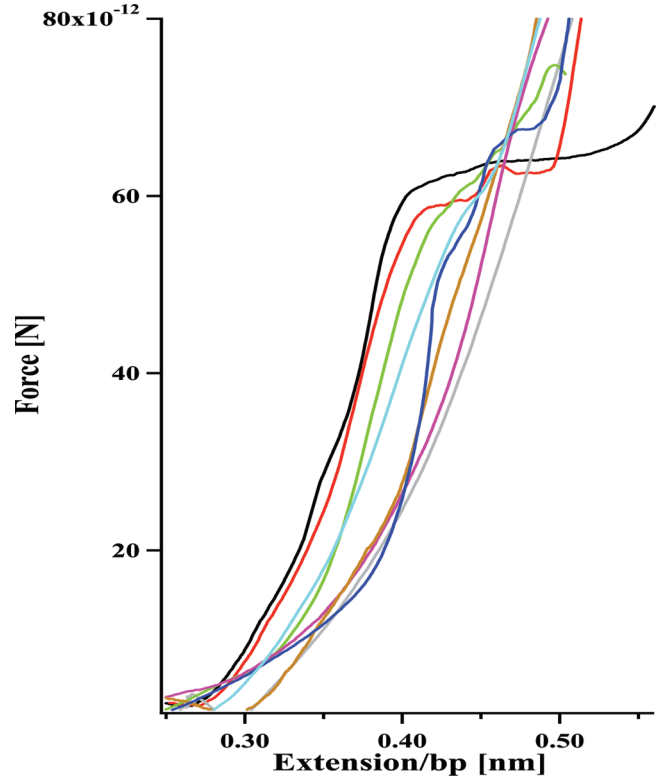

Figure 6. Force extension curves at different concentrations of RDC11. For DNA alone (black) and with the addition of various concentrations of RDC11: 5 (red), 40 (red), 100 (light blue), 400 (dark blue), 1000 (orange), 3000 (violet), and 4000 nM (gray).

of salt. Because the high value of the site size is puzzling, we work on longer DNA to check the affinities and the nature of interaction.

Optical Trapping. Varying the concentration of RDC in solution, we obtained a force−extension for dsDNA at the given concentration of RDC11 (Figure 6). With these curves, we saw that at low forces applied (below 10 pN) and low ruthenium concentration added, the length of the DNA does not change. At higher concentrations of ruthenium from 40 nM to 4 μM, the DNA length is increased. The same behavior was observed at higher forces ($F > 10$ pN). As the concentration of RDC increases, we also observe the loss of the plateau around 62 pN. This plateau is a manifestation of a transition between two structures in the DNA conformation (B→S).[62] Therefore, as RDC11 interacted with DNA, we observed two typical signatures: an increase in the DNA length and a slow loss of the transition while RDC11 concentration increased. These signatures are clearly attributed to an intercalation interaction.

Using the eq 5 to analyze the curves and measure DNA lengths at forces ranging from 20 to 50 pN, by steps of 10 pN, we built Figure 7A. This plot represents the relative extension of the DNA length as a function of RDC11 concentration at different forces. The adjustment of these curves with eq 6 allowed us to to find the affinity constant at each force and the occupancy size in DNA base pairs. We could then adjust K_F (Figure 7B) with eq 7 to find the association constant at zero force, K_0, in which our single molecule stretching experiment is at the order of 5.27×10^6 M^{-1} and the binding site of RDC11 (Figure 7C) varies from 4.5 to 3.5. We could also extract the variation in free energy. In Table 1, we represent the summary of the different results that we found using both bulk analysis with the FRET experiments and the single molecule stretching experiments. We compared our results to those of ruthenium

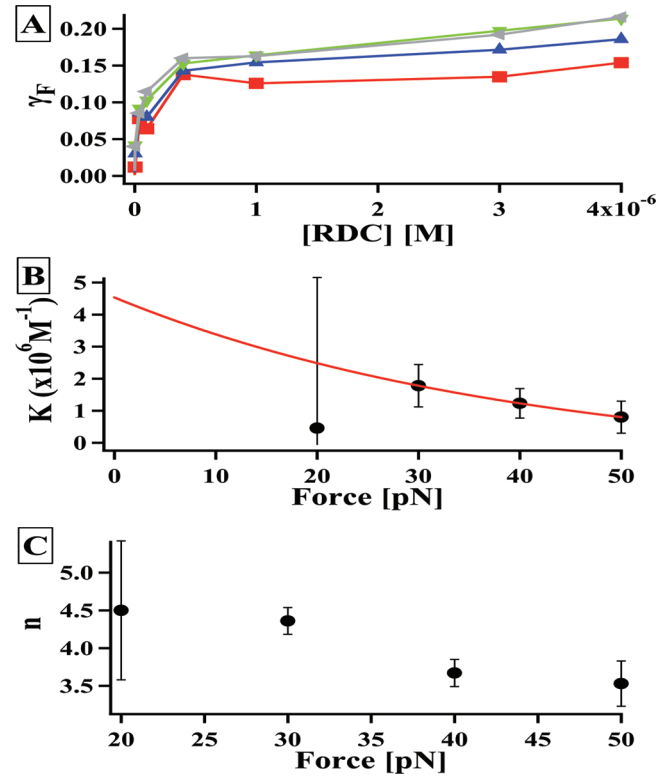

Figure 7. Analysis of the force extension curves. (A) Occupancy fraction of RDC as a function of the concentration under different loads. The squares weare obtained at 20 pN, triangles at 30 pN, circles at 40 pN, and the rhombus at 50 pN. (B) Apparent affinity constant at the different loads, and the exponential fit gives us the affinity constant at rest. (C) Binding site size as a function of the applied load.

TABLE 1: Thermodynamic Parameters for Two Different Types of Ruthenium Compounds[a]

product	experiment	K_0 (M^{-1})	$-\Delta G/k_BT$	$n_{F=0}$	$n_{F=20}$
RDC11 in 10^{-3} mM NaCl	optical trap	5.27×10^6	18.27		4.5
	FRET	1.53×10^6	14.2	8	
$Ru(phen)_2dppz^{2+}$ in 100 mM NaCl	optical trap	9×10^5	13.7		2.3
	bulk	6.3×10^5	13.4	3	

[a] The values for $Ru(phen)_2dppz^{2+}$ are extracted from Vladescu et al.[63]

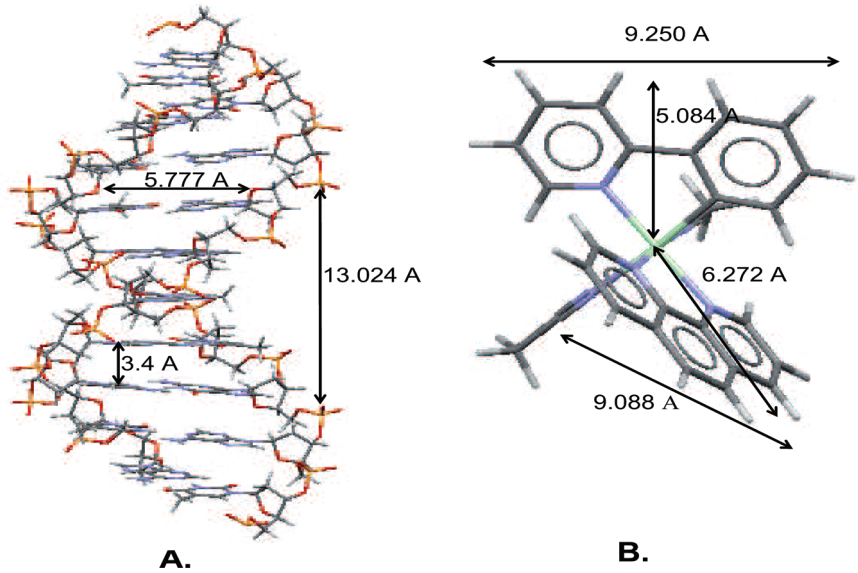

Figure 8. Molecular modeling. (A) Represents B-DNA with the sizes of the minor and major grooves and the interbase distance. (B) Represents RDC11 molecule with the sizes of the two biggest ligands.

compound that have been established in the same way for single molecules and in bulk.

Discussion

We performed two different experiments to answer three complementary question about the interaction mode of RDC11 with DNA.

Determination of the Complex Conformation. The size and the spatial conformation of the complexant molecule control its mode of interaction with DNA strands.[64] As shown in Figure 8, RDC11 molecules possess a phenanthroline group, which has the right dimension to be an intercalator group and a *C*,*N*-(2-phenyl-pyridine) group, that is a good candidate to be a groove binder. It was indeed observed[19,64] that the binding mode of RDC molecules adopts both complexation modes: intercalation or groove binding. In our case, the situation is simpler, at least at the conformation point of view; our main observation was an increase of the DNA contour length from which we must conclude that RDC11 intercalates between DNA base pairs.[53]

Determination of the Thermodynamic Parameters of Interaction. The measurements (FRET and single molecule manipulation) allowed us to obtain the affinity constant of RDC11 with DNA. We measured the same affinity $K_a \simeq 5 \times 10^6$ M^{-1} whatever the DNA length. This agreement between the two techniques shows that the DNA length (from 15 bp to 8.6 kbp) does not play a role on the affinity of RDC11 with DNA.

Description of the Molecular Mechanism of Interaction. FRET experiments showed that the affinity constant decreases with the addition of salt. Thus, although intercalation occurs, in which hydrogen bonds and hydrophobic forces play the most important role,[65,66] electrostatic interactions still play an important role. On the other hand, mechanical measurements that enable fine probing of the potential energy landscape between DNA and RDC11 showed a dependence of the affinity on the applied force: The affinity decreases when DNA is pulled. This result is at odds with previous measurements of the change of affinity under tension. When one pulls DNA, the distance between the base pairs increases, and as a consequence, lower reaction energies are necessary, and the affinity is observed to increase[63] if only sterical interactions are needed. In our case, the interactions are decreasing with force, and we have to assume that another energy must be taken into account to explain this behavior.

It cannot be explained by the change in the electrostatic interaction between DNA and RDC. Indeed, in the absence of force, the distance between two base pairs is 3.4 Å, whereas the Bjerrum length is 7 Å. Thus, according to Manning condensation theory,[67] only half of DNA base pairs phosphate is dissociated. When DNA is pulled, the DNA base pair distance increased up to 4.5 Å and remained lower than the Bjerrum length. As a consequence, the lineic charge of DNA remains constant [and equal to $(1/7) \times 1.6 \times 10^{-19}$ C Å $^{-1}$] and the electrostatic interactions when DNA is stretched. So when pulling on DNA, one must be sensitive to another energy than the coulombian one.

We assume that while stretching DNA, the interbase distance increases. As a consequence, the hydrogen bonds and hydrophobic interactions with the complexant lower. When RDC11 gets into the base stacking, it is less isolated from the surrounding medium, and the hydrogen bonds are further lowering its affinity with DNA at higher forces, which may be responsible for the decrease of the affinity with tension.

Acknowledgment. M.K. is grateful for financial support from the Alsace Region and the Marshall of Lower Silesia. C.G. is grateful for financial support from La Ligue contre le Cancer, ARC and INCA. We acknowledge the CNRS for funding this research. We thank Dr. Michael Guy Poirier for the discussions and his questions about the understanding of the intrinsic mechanism. We thank especially Dr. Alexandre Boeglin for helpful proofreading of the manuscript and interesting discussions about the different possible interactions.

References and Notes

(1) Rosenberg, B.; Van Camp, L.; Krigas, T. *Nature* **1965**, *205*, 698–699.
(2) Rosenberg, B.; Van Camp, L.; Trosko, J.; Mansour, V. *Nature* **1969**, *222*, 385–386.
(3) Rougier, P.; Zarba, J.; Ducreux, M.; Basile, M.; Pignon, J.; Mahjoubi, M.; Benahmed, M.; Droz, J.; Cvitkovic, A. J. E. *Ann. Oncol.* **1993**, *4*, 333–336.
(4) Williams, S.; Stablein, D.; Einhorn, L.; Muggia, F.; Weiss, R.; Donohue, J.; Paulson, D.; Brunner, K.; Jacobs, E.; Spaulding, J.; DeWys, W.; Crawford, E. *N. Engl. J. Med.* **1987**, *317*, 1433–1438.
(5) Alberts, D.; Liu, P.; Hannigan, E.; O'Toole, R.; Williams, S.; Young, J.; Franklin, E.; Clarke-Pearson, D.; Malviya, V.; DuBeshter, B.; Adelson, M.; Hoskins, W. *N. Engl. J. Med.* **1996**, *335*, 1950–1955.
(6) Wong, E.; Giandomenico, C. *Chem. Rev.* **1999**, *99*, 2451–2466.
(7) Stuart, N.; Woodroffe, C.; Grundy, R.; Cullen, M. *Br. J. Cancer* **1990**, *61*, 479–484.
(8) Coates, A.; Abraham, S.; Kaye, S.; Sowerbutts, T.; Frewin, C.; Fox, R.; Tattersall, M. *Eur. J. Cancer Clin. Oncol.* **1983**, *19*, 203–208.
(9) Lane, B.; Smith, A.; Larson, B.; Gong, M.; Campbell, S.; Raghavan, D.; Dreicer, R.; Hansel, D.; Stephenson, A. *Cancer* **2010**, *116*, 2967–2973.
(10) Sonpavde, G.; Goldman, B.; Speights, V.; Lerner, S.; Wood, D.; Vogelzang, N.; Trump, D.; Natale, R.; Grossman, H.; Crawford, E. *Cancer* **2009**, *115*, 4104–4109.
(11) Morris, R.; Aird, R.; Murdoch, P.; Chen, H.; Cummings, J.; Hughes, N.; Parsons, S.; Parkin, A.; Boyd, G.; Jodrell, D.; Sadler, P. *J. Med. Chem.* **2001**, *44*, 3616–3621.
(12) Yan, Y.; Melchart, M.; Habtemariam, A.; Sadler, P. *Chem. Commun.* **2005**, 4764–4776.
(13) Aird, R.; Cummings, J.; Ritchie, A.; Muir, M.; Morris, R.; Chen, H.; Sadler, P.; Jodrell, D. *Br. J. Cancer* **2002**, *86*, 1652–1657.
(14) Novakova, O.; Chen, H.; Vrana, O.; Rodger, A.; Sadler, P.; Brabec, V. *Biochemistry* **2003**, *42*, 11544–11554.
(15) Galanski, M.; Arion, V.; Jakupec, M.; Keppler, B. *Curr. Pharm. Des.* **2003**, *9*, 2078–2089.
(16) Smith, C.; Sutherland-Smith, A.; Keppler, B.; Kratz, F.; Baker, E. *J. Biol. Inorg. Chem.* **1996**, *1*, 424–431.
(17) Meng, X.; Leyva, M. L.; Jenny, M.; Gross, I.; Benosman, S.; Fricker, B.; Harlepp, S.; Hebraud, P.; Boos, A.; Wlosik, P.; Bischoff, P.; Sirlin, C.; Pfeffer, M.; Loeffler, J.-P.; Gaiddon, C. *Cancer Res.* **2009**, *69*, 5458–5466.
(18) Giovagnini, L.; Sitran, S.; Castagliuolo, I.; Brun, P.; Corsini, M.; Zanello, P.; Zoleo, A.; Maniero, A.; Biondia, B.; Fregona, D. *Dalton Trans.* **2008**, *47*, 6699–6708.
(19) Han, M.; Gao, L.; Lu, Y.; Wang, K. *J. Phys. Chem. B* **2006**, *110*, 2364–2371.
(20) Bergamo, A.; Gava, B.; Alessio, E.; Mestroni, G.; Serli, B.; Cocchietto, M.; Zorzet, S.; Sava, G. *Int. J. Oncol.* **2002**, *21*, 1331–1338.
(21) Scolaro, C.; Bergamo, A.; Brescacin, L.; Delfino, R.; Cocchietto, M.; Laurenczy, G.; Geldbach, T.; Sava, G.; Dyson, P. *J. Med. Chem.* **2005**, *48*, 4161–4171.
(22) Sava, G.; Giraldi, T.; Mestroni, G.; Zassinovich, G. *Chem.-Biol. Interact.* **1983**, *45*, 1–6.
(23) Fruhauf, S.; Zeller, W. *Cancer Res.* **1991**, *51*, 2943–2948.
(24) Novakova, O.; Kasparkova, J.; Vrana, O.; Vanlviet, P.; Reedjik, J.; Brabec, V. *Biochemistry* **1995**, *34*, 12369–12378.
(25) Allardyce, C.; Dyson, P.; Ellis, D.; Heath, S. *Chem. Commun.* **2001**, *15*, 1396–1397.
(26) Bruijnincx, P.; Sadler, P. *Curr. Opin. Chem. Biol.* **2008**, *12*, 197–206.
(27) Frasca, D.; Clarke, M. *J. Am. Chem. Soc.* **1999**, *121*, 8523–8532.
(28) Hambley, T. *Science* **2007**, *318*, 1392–1393.
(29) Xu, H.; Zheng, K.; Chen, Y.; Li, Y.; Lin, L.; Li, H.; Zhang, P.; Ji, L. *Dalton Trans.* **2003**, *11*, 2260–2268.
(30) Kartalou, a. E. J. M. *Mutat. Res., Fundam. Mol. Mech. Mutagen.* **2001**, *478*, 23–43.
(31) Garzon, F.; Berger, M.; Keppler, B.; Schmahl, D. *Cancer Chemother. Pharmacol.* **1987**, *19*, 347–349.
(32) Sava, G.; Pacor, S.; Zorzet, S.; Alessio, E.; Mestroni, G. *Pharmacol. Res.* **1989**, *21*, 617–628.
(33) Mihailovic, A.; Vladescu, L.; McCauley, M.; Ly, E.; Williams, M.; Spain, E.; Nunez, M. *Langmuir* **2006**, *22*, 4699–4709.
(34) Mei, H.; Barton, J. *Proc. Natl. Acad. Sci.* **1988**, *85*, 1339–1343.
(35) Brabec, V. *Prog. Nucleic Acid Res. Mol. Biol.* **2002**, *71*, 1–68.
(36) Smith, S.; Finzi, L.; Bustamante, C. *Science* **1992**, *258*, 1122–1126.
(37) Zwelling, L. A.; Anderson, T.; Kohn, K. W. *Cancer Res.* **1979**, *39*, 365–369.
(38) Menetski, J. P.; Kowalczykowski, S. C. *J. Mol. Biol.* **1985**, *181*, 281–295.
(39) Gaiddon, C.; Jeannequin, P.; Bischoff, P.; Pfeffer, M.; Sirlin, C.; Loeffler, J. *J. Pharmacol. Exp. Ther.* **2005**, *315*, 1403–1411.
(40) Leyva, L.; Sirlin, C.; Rubio, L.; Franco, C.; Le Lagadec, R.; Spencer, J.; Bischoff, P.; Gaiddon, C.; Loeffler, J.-P.; Pfeffer, M. *Eur. J. Inorg. Chem.* **2007**, 3055–3066.
(41) Coury, J.; McFailIsom, L.; Williams, L.; Bottomley, L. *Proc. Natl. Acad. Sci.* **1996**, *93*, 12283–12286.
(42) Saito, M.; Kobayashi, M.; Iwabuchi, S.; Morita, Y.; Takamura, Y.; Tamiya, E. *J. Biochem.* **2004**, *136*, 813–823.
(43) Adamcik, J.; Valle, F.; Witz, G.; Rechendorff, K.; Dietler, G. *Nanotechnology* **2008**, *19*, 1–7.
(44) Jares-Erijman, E. A.; Jovin, T. M. *J. Mol. Biol.* **1996**, *257*, 597.
(45) Clegg, R. M.; Murchie, A. I. H.; et al. *Proc. Natl. Acad. Sci.* **1994**, *91*, 11660.
(46) Ying, L.; Green, J. J.; et al. *Proc. Natl. Acad. Sci.* **2003**, *100*, 14629.
(47) Lilley, D. M.; Clegg, R. M. *Q. Rev. Biophys.* **1993**, *26*, 131–175.
(48) Grunwell, J. R.; Glass, J. L.; Lacoste, T. D.; Deniz, A. A.; Chemla, D. S.; Schultz, P. G. *J. Am. Chem. Soc.* **2001**, *123*, 4295.
(49) Murphy, M. C.; Rasnik, I.; Cheng, W.; Lohman, T. M.; Ha, T. *Biophys. J.* **2004**, *86*, 2530.
(50) Tuschl, T.; Gohlke, C.; Jovin, T. M.; Westhof, E.; Eckstein, F. *Science* **1994**, *266*, 785.
(51) Weiss, J. *FASEB J.* **1997**, *11*, 835–841.
(52) Iqbal, A.; Arslan, S.; Okumus, B.; Wilson, T. J.; Giraud, G.; Norman, D. G.; Ha, T.; Lilley, D. M. J. *Proc. Natl. Acad. Sci.* **2008**, *105*, 11176–11181.
(53) Sischka, A.; Toensing, K.; Eckel, R.; Wilking, S.; Sewald, N.; Ros, R.; Anselmetti, D. *Biophys. J.* **2005**, *88*, 404–411.
(54) Baumann, C. G.; Bloomfield, V. A.; Smith, S. B.; Bustamante, C.; Wang, M. D.; Block, S. M. *Biophys. J.* **2000**, *78*, 1965–1978.
(55) Wang, M.; Yin, H.; Landick, R.; Gelles, J.; Block, S. *Biophys. J.* **1997**, *72*, 1335–1346.
(56) Jamieson, E. R.; Lippard, S. J. *Chem. Rev.* **1999**, *99*, 2467–2498.
(57) http://www.invitrogen.com/site/us/en/home/References/Molecular-Probes-The-Handbook/tables/R0-values-for-some-Alexa-Fluor-dyes.html.
(58) Scatchard, S. *Ann. N. Y. Acad. Sci.* **1949**, *51*, 660–672.
(59) McGhee, J. D.; Hippel, P. H. V. *J. Mol. Biol.* **1974**, *86*, 469–489.
(60) Baumann, C. G.; Smith, S. B.; Bloomfield, V. A.; Bustamante, C. *Proc. Natl. Acad. Sci.* **1997**, *94*, 6185–6190.
(61) Braunlin, W. H.; Strick, T. J.; Record, M. T., Jr. *Biopolymers* **1982**, *21*, 1301–1314.
(62) Cluzel, P.; Lebrun, A.; Heller, C.; Lavery, R.; Viovy, J.-L.; Chatenay, D.; Caron, F. *Science* **1996**, *271*, 792–794.
(63) Vladescu, I. D.; McCauley, M. J.; Nunez, M. E.; Rouzina, I.; Williams, M. C. *Nature Methods* **2007**, *4*, 517–522.
(64) Zeglis, B. M.; Pierre, V. C.; Barton, J. K. *Chem. Commun.* **2007**, *44*, 4549–4696.
(65) Kellogg, G.; Scarsdale, J.; Fornari, F. A. *Nucleic Acids Res.* **1998**, *26*, 4721–4732.
(66) McMillin, D. R.; Shelton, A. H.; Bejune, S. A.; Fanwick, P. E.; Wall, R. K. *Coord. Chem. Rev.* **2005**, *249*, 1451–1459.
(67) Manning, G. *J. Chem. Phys.* **1969**, *51*, 924–933.

JP1044783